JOURNAL OF CHEMICAL & ENGINEERING DATA

ARTICLE

pubs.acs.org/jced

A Monte Carlo Study of the Structure of a Planar Electric Double Layer Containing Asymmetric Electrolytes

Lutful Bari Bhuiyan

Laboratory of Theoretical Physics, Department of Physics, University of Puerto Rico, Box 70377, San Juan, Puerto Rico 00936-8377

Christopher W. Outhwaite

Department of Applied Mathematics, University of Sheffield, S3 7RH, United Kingdom

Douglas Henderson*

Department of Chemistry and Biochemistry, Brigham Young University, Provo, Utah 84602-5700, United States

ABSTRACT: During our recent simulation studies of the contact values of the density and charge profiles formed by symmetric and asymmetric electrolytes near charged electrodes, we have accumulated a large number of Monte Carlo (MC) simulation results for ionic distribution profiles as a function of the distance of the ions from the electrode. The ions were modeled as charged hard spheres in a dielectric continuum whose dielectric constant equals that of the solvent (the primitive model), while the electrode was modeled as a hard unpolarized uniformly charged planar surface. Some of the density and potential profiles for this model system for electrolytes with one or both asymmetric in charge and size for varying electrolyte concentrations and electrode charge densities are reported here. These simulations are used to assess the results of (i) the classical Poisson−Boltzmann (PB) theory, (ii) a simplified extension of the Poisson−Boltzmann theory, called PB+EVT, that includes excluded volume effects but neglects ion correlations beyond those provided by the charge interactions, and (iii) in the case of charge asymmetry but symmetric size, the modified Poisson−Boltzmann (MPB) theory. The PB results are rather poor, whereas the MPB results are quite good. At low concentrations, the PB+EVT results are nearly the same as the PB results. However, some improvement is seen at higher concentrations.

INTRODUCTION

The diffuse electric double layer formed by an electrolyte near a charged surface or electrode is of experimental interest in electro/analytical chemistry and of engineering interest in diverse fields such as corrosion, fuel cell technology, and biophysical applications (viz., ionic channels), besides being of theoretical interest. The electrolyte can normally be treated at the classical level using statistical mechanics, but for the electrode the quantum mechanical effects can be important. For a metallic electrode the excess charge arising from the electrons in the electrode is confined to a very small surface thickness, so that the metal can be treated as a structureless classical metal with zero skin depth and with all of the charge of the electrode residing on its surface. Polarization effects can be readily treated in the classical model; see the recent simulation study of Nagy et al.[1] of charge asymmetric ions in the Prausnitz issue of this journal and the references cited therein.

The classical Poisson−Boltzmann (PB) theory for binary symmetric electrolytes, commonly known in the double layer literature as the Gouy−Chapman−Stern (GCS) theory,[2−4] is widely used to interpret experimental results for the electrochemical properties of double layers formed by low concentration electrolytes and weakly charged electrodes. The main reason for its widespread use is that it can yield analytic results and not because it is particularly accurate. In fact, it can be rather inaccurate, and its results vary widely depending upon whether the electrode charge or potential is used as the independent variable. At least for symmetric electrolytes, the GCS theory is most accurate when the electrode charge is used, which is a point of logical interest because the potential is really the more natural independent variable of the theory. When the ions are asymmetric in diameter, we refer to the PB theory as the modified GCS or MGCS theory because the theory was developed originally for symmetric electrolytes, especially for ions with the same size. When the ions are not all of equal size, there is not a single distance of closest approach to the electrode.

The model of the electrolyte that underlies the MGCS theory is the *primitive model* (PM) in which the ions are treated as charged spheres and the solvent (usually water) is treated as a dielectric continuum whose dielectric constant equals that of the solvent. When the charged hard spheres are all of the same diameter, this model is called the *restricted primitive model* (RPM). The electrode is modeled as an impenetrable, smooth, unpolarized, uniformly charged plane with all of the electrode charge located on the surface. In the MGCS theory, correlations between the ions are neglected; the wall−ion correlations are treated at a simple level by taking note of their distance of closest approach to the electrode. The MGCS theory yields analytic results for the RPM (all ions have the same distance of closest

Special Issue: Kenneth N. Marsh Festschrift

Received: May 27, 2011
Accepted: July 16, 2011
Published: August 05, 2011

approach) and for binary electrolytes in which the ions all have the same magnitude of charge[5] or when the magnitude of their charge ratio is 2:1.[6] For other single salt RPM applications or PM situations, the MGCS theory does not yield simple closed form analytic results, and the equations, although not overly complex, must be solved numerically.

With few exceptions, more modern theories that can be applied to the study of the electric double layer seem to fall into two classes. They are either relatively easy to employ and are improvements over the MGCS theory but not really satisfactory, or they are very accurate but extremely difficult computationally. Examples of the first class are the mean spherical[7] and hypernetted chain approximations.[8,9] Examples of the second class are the second-order versions of these theories.[10−13] More recently, field theoretical methods have also been tried.[14,15] The density functional theory (DFT) has also seemed to be a promising approach (see for example, some recent papers by Boda et al.,[16] Gillespie et al.,[17,18] Valiskó et al.,[19] Wang et al.,[20] Yu et al.,[21] and a related work[22]). Other very recent relevant publications on the double layer include those by Martin-Molina et al.,[23] Gerrero-Garcia et al.,[24] and Kiyohara et al.[25] These works reveal the continued broad interest in the double-layer phenomenon. One theory that is fairly straightforward to employ but still quite accurate and has been successful across planar, spherical, and cylindrical geometries is the modified Poisson−Boltzmann (MPB) theory.[26−29] A simple version of the MPB approach that includes excluded volume (or ion size effects) but not the fluctuation potential effects is the PB+EVT approach.[30,31]

The most obvious reliable approach, but certainly not as convenient as a formal analytic theory, is the use of simulations. These are usually canonical Monte Carlo (MC) simulations, but grand canonical Monte Carlo (GCMC) and molecular dynamics (MD) have also been used. The MC simulations of the double layer started with the seminal papers of Torrie and Valleau.[32,33] More recent simulations have been initiated by Boda et al.[34,35] and Lamperski and Bhuiyan.[36] Recently, we have conducted an extensive set of simulations of the double layers formed by symmetric electrolytes,[37−39] electrolytes that are asymmetric in charge,[40] in size,[41] or in both charge and size.[42] The goal of these simulations was to test a semiempirical expression for the contact value of the difference (or charge) profile,[43] which was found to be reasonably accurate. The principal aim of this paper is to present some of our simulation results for the co-ion, counterion, and potential profiles across the whole of the double layer and not just their contact values. We will also use the simulations to compare the corresponding predictions from the GCS (or MGCS), the PB+EVT, and the MPB theories where relevant.

MODEL, SIMULATIONS, AND THEORY

We have employed here the PM binary electrolyte where the ions of species i are taken to be charged hard spheres of diameter d_i and charge $z_i e$, with e being the magnitude of the elementary charge and z_i the valence. The solvent is considered to be a dielectric continuum characterized by a single dielectric constant (relative permittivity) ε_r, whose value in the present case is taken to be 78.5, typical for a water-like solvent. We have chosen the ion diameters in such a way that the average diameter $d = (d_{co} + d_{ctr})/2 = 4.25 \cdot 10^{-10}$ m, a value used by Torrie and Valleau.[32,33] The subscripts "co" and "ctr" refer to co- and counterions, respectively. We have restricted ourselves to binary electrolytes with the values of $|z_i|$ used being 1 or 2. The model electrode employed is an unpolarized, uniformly charged hard plane with a surface charge density of σ.

Monte Carlo Simulations. The MC simulations were performed in the canonical ensemble ((N,V,T) ensemble) using the well-known and standard Metropolis algorithm. The techniques were similar to those employed by Boda et al.[34,35] and Lamperski and Bhuiyan.[36] The MC cell was a rectangular parallelepiped with edges l_x, l_y, and l_z with one of the yz faces mimicking the planar electrode at $x = 0$, while the other at $x = l_x$ is uncharged. The ionic exclusion surfaces parallel to the yz faces were determined by the ionic radii of the species. A convenient way to ensure this was to make the difference of the two radii to be some whole multiple of the "bin" size. The periodic boundary conditions along the minimum image method along y and z directions accounted for the semi-infinite nature of the system, while the charged sheets method of Torrie and Valleau[32] was invoked to address the issue of the long-range nature of the electrostatic interactions. The latter procedure has been improved by Boda et al.[44] Within the canonical ensemble simulation, the target bulk concentration was achieved by an adjustment of the cell length l_x. We typically sampled configurations of the order 10^7, out of which $\sim 10^6$ were used to equilibrate the system. The statistical uncertainty in reproducing the bulk concentration was about ± 2 %.

Modified Poisson−Boltzmann (MPB) and the Exclusion Volume Corrected Poisson−Boltzmann (PB+EVT) Theories. The MPB approach to the double layer theory seeks to improve upon the classical PB theory, within a potential formulation, by accounting for the neglected fluctuation potential and ionic exclusion volume effects. To date the most successful formulation of the MPB theory is at the MPB5 level, which has been utilized in the present work. The development of the MPB5 theory for the RPM planar double layer is available elsewhere in the literature (see for example, ref 26). We will therefore content ourselves with a brief outline of the main equations for the planar double layer with no polarization.

The Poisson's equation for the mean electrostatic potential $\psi(x)$ at a perpendicular distance x from the electrode reads

$$\frac{d^2\psi}{dx^2} = -\frac{e}{\varepsilon_0 \varepsilon_r} \sum_s z_s \rho_s g_s(x) \tag{1}$$

with ε_0 as the vacuum permittivity and ρ_s the mean number density of ions species s. In the MPB theory, in conjunction with the Kirkwood charging process, the electrode−ion distribution function $g_s(x)$ is given by

$$g_s(x) = \xi_s(x) \exp\left[-z_s e\beta L(\psi) - \frac{\beta z_s^2 e^2}{8\pi\varepsilon_0\varepsilon_r d}(F - F_0)\right] \tag{2}$$

Note that $\beta = 1/(k_B T)$, k_B is the Boltzmann constant and T the absolute temperature. The quantity $\xi_s(x) = g_s(x|z_s = 0)$ is the exclusion volume term. Also,

$$L(\psi) = \frac{F}{2}\{\psi(x + d) + \psi(x - d)\} - \frac{(F-1)}{2d}\int_{x-d}^{x+d} \psi(y)\, dy \tag{3}$$

$$F = \frac{4}{4 + \kappa(d + 2x)} \qquad d/2 \le x \le 3d/2$$
$$= \frac{1}{(1 + \kappa d)} \qquad x \ge 3d/2 \tag{4}$$

dx.doi.org/10.1021/je2005193 |J. Chem. Eng. Data 2011, 56, 4556–4563

$$\kappa^2 = \frac{\beta e^2}{\varepsilon_0 \varepsilon_r} \sum_s z_s^2 \rho_s g_s(x) \tag{5}$$

$$\kappa_0 = \lim_{x \to \infty} \kappa \tag{6}$$

$$F_0 = \lim_{x \to \infty} F = \frac{1}{1 + \kappa_0 d} \tag{7}$$

In the above equations d is the common ionic diameter in the RPM. The exclusion volume term is developed through the Bogoliuobov−Born−Green−Yvon (BBGY) hierarchy,

$$\xi_s(x) = H(x - d/2) \exp\left[-2\pi \int_\infty^x \sum_t \cdot \rho_t \cdot \int_{\max(d/2, y-d)}^{y+d} (y' - y) g_t(y') g_{st}(d) \cdot \exp\{-\beta z_t e \Phi(1; 2|z_s = 0, r_{12} = d)\} dy' dy\right] \tag{8}$$

Here $H(x)$ is the Heaviside function, $\Phi(x)$ is the fluctuation potential, and $g_{is}(d) = g(d)$ is the pair distribution function at contact given by[45]

$$g(d) = \frac{2 - \eta}{2(1 - \eta)^3} \tag{9}$$

with the packing fraction $\eta = (\pi/6) d^3 \Sigma_s \rho_s$.

The classical GCS theory follows by neglecting the fluctuation and exclusion volume terms, that is, substituting in eq 2 $L(\psi) = \psi$, $F = F_0$, and $\xi_s = H(x - d/2)$. If however, only the fluctuation potential is neglected, then the PB+EVT theory follows, where the electrode−ion distribution is now

$$g_s(x) = \xi_s(x) \exp(-e\beta z_s \psi(x)) \tag{10}$$

We note that in the absence of the fluctuation potential the expression for $\xi_s(x)$ (eq 8) can be simplified to

$$\xi_s(x) = H(x - d) \exp\left\{\pi \sum_t \rho_t g_{st}(d) \cdot \left[\int_{\max(d/2, x-d)}^{x+d} [(y - x)^2 - d^2] g_t(y) dy + 4d^3/3\right]\right\} \tag{11}$$

In case of unequal ion diameters $\xi_s(x)$ can be written in the form

$$\xi_s(x) = H(x - d_s/2) \exp\{B_s(x) + (4\pi/3) \sum_t \rho_t g_{st}(d_{st}) d_{st}^3\} \tag{12}$$

$$B_s(x) = \pi \sum_t \rho_t g_{st}(d_{st}) \int_{\max(d_t/2, x-d_{st})}^{x+d_{st}} [(y - x)^2 - (d_{st}/2)^2] g_t(y) dy \tag{13}$$

where $d_{st} = (d_s + d_t)/2$. The pair distribution functions at contact, $g_{st}(d_{st})$, are approximated by the corresponding Percus−Yevick values.[46]

In passing, we remark that the MC result for the potential profile $\psi_{MC}(x)$ was obtained from a direct integration of the MC

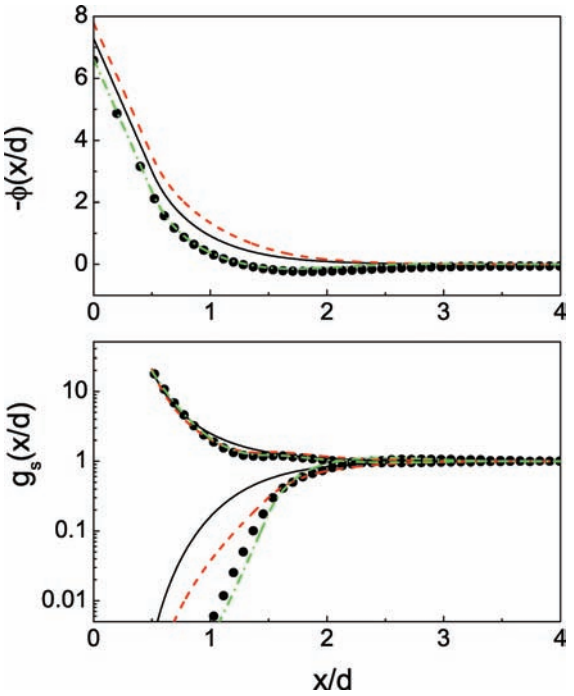

Figure 1. Mean electrostatic potential $\phi(x/d)$ and the electrode−ion singlet distribution functions $g_s(x/d)$ in a 1^+:2^- RPM planar double layer at $\rho^* = 0.139$ ($c = 1$ mol·dm^{-3}), $T^* = 0.297$ ($T = 298$ K), $b = 5$, and $\sigma^* = -0.405$ ($\sigma = -0.359$ C·m^{-2}). Symbols, MC simulation data; solid line, GCS result; dashed line, PB+EVT result; and dash−dotted line, MPB result.

$g_s^{MX}(x)$, namely,

$$\psi_{MC}(x) = -\frac{e}{\varepsilon_0 \varepsilon_r} \sum_s \rho_s z_s \int_x^\infty (t - x) h_s^{MC}(t) dt \tag{14}$$

$$h_s(x) = g_s(x) - 1 \tag{15}$$

The MPB and the PB+EVT equations were solved by a previously developed quasi-linearization iterative technique,[47] while the MGCS theory has an analytic solution for 1:2/2:1 valency systems.[6]

RESULTS

The MC simulations and the corresponding GCS (or MGCS), PB+EVT, and MPB calculations were done at the mean diameter $d = 4.25 \cdot 10^{-10}$ m, relative permittivity $\varepsilon_r = 78.5$, and two different radius ratios $\alpha = (d_+/d_-) = 0.308$ and 0.545. The salt concentration varied from 0.2 mol·dm^{-3} to 1 mol·dm^{-3}. Although the temperature was taken to be $T = 298$ K for all the unequal radii cases, a different value $T = 150$ K was used in one of the RPM situations. These physical parameters are the same as in the earlier papers.[37−42] We will discuss the results in terms of universal reduced quantities for convenience. The relevant ones are the reduced density ρ^*, the reduced temperature T^*, and the reduced surface charge σ^*, defined as follows.

$$\rho^* = \rho_{co} d_{co}^3 + \rho_{ctr} d_{ctr}^3 = \rho d^3 \left[\left(\frac{\rho_{co}}{\rho}\right)\left(\frac{d_{co}}{d}\right)^3 + \left(\frac{\rho_{ctr}}{\rho}\right)\left(\frac{d_{ctr}}{d}\right)^3\right] \tag{16}$$

dx.doi.org/10.1021/je2005193 |J. Chem. Eng. Data 2011, 56, 4556–4563

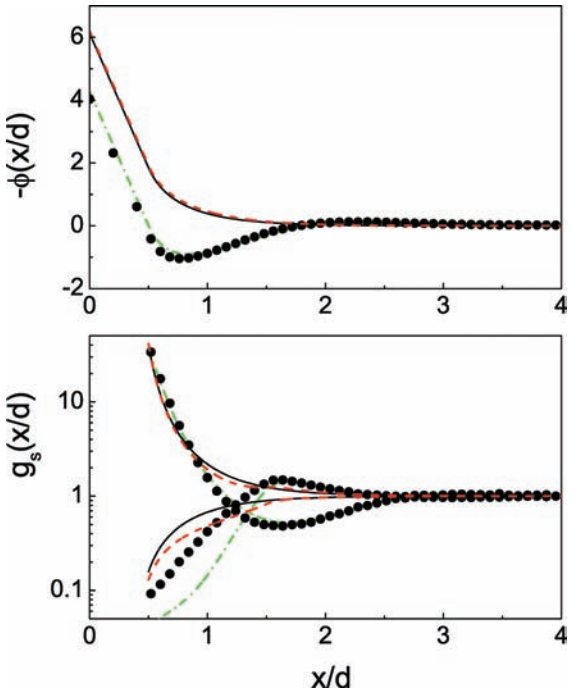

Figure 2. Mean electrostatic potential $\phi(x/d)$ and the electrode−ion singlet distribution functions $g_s(x/d)$ in a 2^+:1^- RPM planar double layer at ρ^* =0.139 (c = 1 mol·dm^{-3}), T^* = 0.297 (T = 298 K), b = 5, and σ^* = −0.405 (σ = −0.359 C·m^{-2}). Notation as in Figure 1.

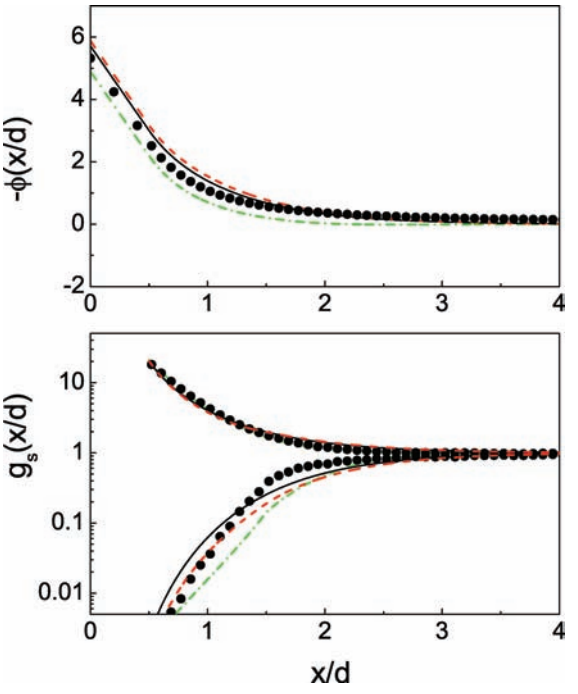

Figure 3. Mean electrostatic potential $\phi(x/d)$ and the electrode−ion singlet distribution functions $g_s(x/d)$ in a 1^+:2^- RPM planar double layer at ρ^* =0.0277 (c = 0.2 mol·dm^{-3}), T^* = 0.150 (T = 150 K), b = 5, and σ^* = −0.129 (σ = −0.114 C·m^{-2}). Notation as in Figure 1.

$$T^* = \frac{4\pi\varepsilon_0\varepsilon_r k_B T d}{-z_{co}z_{ctr}e^2} \tag{17}$$

$$\sigma^* = \frac{\sigma d^2}{e} \tag{18}$$

where $\rho = \rho_{co} + \rho_{ctr}$. In eq 16, the quantity ρd^3 is the reduced density in the RPM limit so that the equation relates the ρ^* in the PM and the RPM at the same solution concentration. In our study it was also convenient to use $b = (-z_{co}z_{ctr})^{1/2}e\sigma/(\varepsilon_0\varepsilon_r k_B T\kappa_0)$ to specify the electrode charge density as this is the natural variable that arises in the contact value expressions. To facilitate viewing both low and high values of the electrode−ion distributions near contact, we have opted to plot these using a logarithmic scale. We would like to note here that a preliminary MPB calculation for unequal radii electrolytes was attempted some time ago by Outhwaite and Bhuiyan.[48] However, the calculations were somewhat limited, and the results have not proved adequate in terms of accuracy. Thus, in this work the MPB results will be presented for RPM systems only.

We begin this discussion by considering some 1:2/2:1 RPM system results shown in Figures 1 to 3, all at b = 5. The profiles in the former two figures are at ρ^* = 0.139 (concentration c = 1 mol·dm^{-3}), σ^* = −0.405 (σ = −0.359 C·m^{-2}), and T^* = 0.297 (T = 298 K). Note also that in Figure 1 the counterions are monovalent, while in Figure 2 they are divalent. In each case there are oscillations in the profiles, which are more prominent in the presence of multivalent counterions (Figure 2). The excess of such counterions near the electrode lead to a deep first minimum in the mean electrostatic potential profile $\phi(x/d)$ suggesting a charge reversal. Here ϕ is the dimensionless mean electrostatic potential defined by $\phi = e\beta\psi$. Clearly, along with the strong Coulomb correlations and exclusion volume effects at high

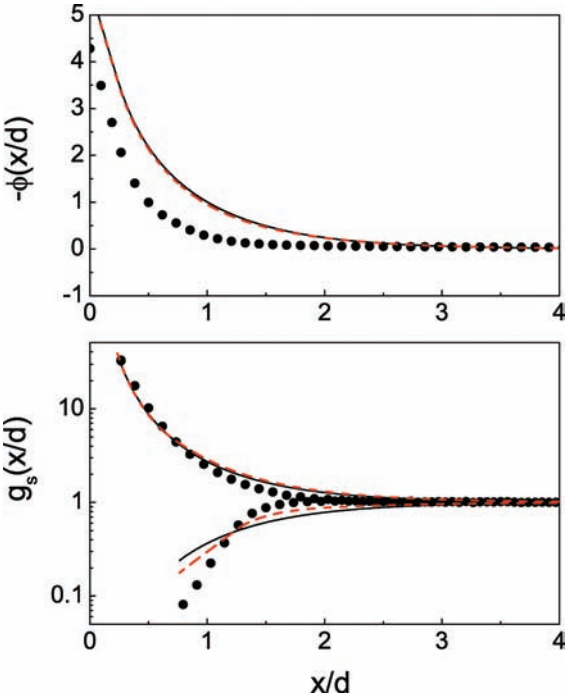

Figure 4. Mean electrostatic potential $\phi(x/d)$ and the electrode−ion singlet distribution functions $g_s(x/d)$ in a 1^+:1^- PM planar double layer at α = 0.308, ρ^* = 0.170 (c = 1 mol·dm^{-3}), T^* = 0.595 (T = 298 K), b = 6, and σ^* = −0.397 (σ = −0.352 C·m^{-2}). Symbols, MC simulation data; solid line, MGCS result; and dashed line, PB+EVT result.

dx.doi.org/10.1021/je2005193 |J. Chem. Eng. Data 2011, 56, 4556–4563

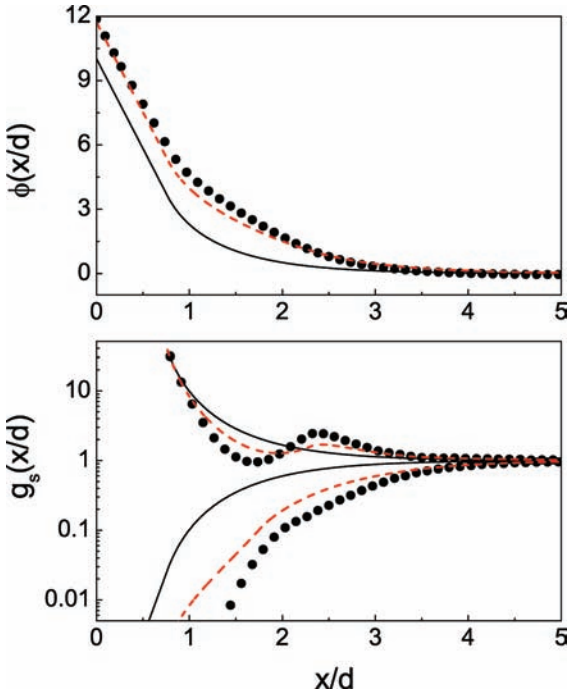

Figure 5. Mean electrostatic potential $\phi(x/d)$ and the electrode−ion singlet distribution functions $g_s(x/d)$ in a 1^+:1^- PM planar double layer at $\alpha = 0.308$, $\rho^* = 0.170$ ($c = 1$ mol·dm^{-3}), $T^* = 0.595$ ($T = 298$ K), $b = 6$, and $\sigma^* = 0.397$ ($\sigma = 0.352$ C·m^{-2}). Notation as in Figure 4.

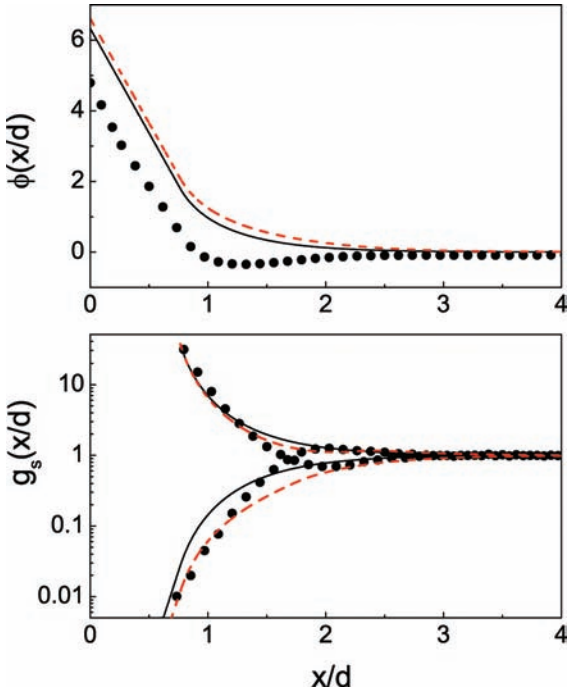

Figure 6. Mean electrostatic potential $\phi(x/d)$ and the electrode−ion singlet distribution functions $g_s(x/d)$ in a 2^+:2^- PM planar double layer at $\alpha = 0.308$, $\rho^* = 0.0851$ ($c = 0.5$ mol·dm^{-3}), $T^* = 0.15$ ($T = 298$ K), $b = 6$, and $\sigma^* = 0.281$ ($\sigma = 0.249$ C·m^{-2}). Notation as in Figure 4.

concentrations, the role of the electrode−counterion interaction is important in shaping the double-layer structure. The physical difference between the model systems in Figures 1 and 2 is in the

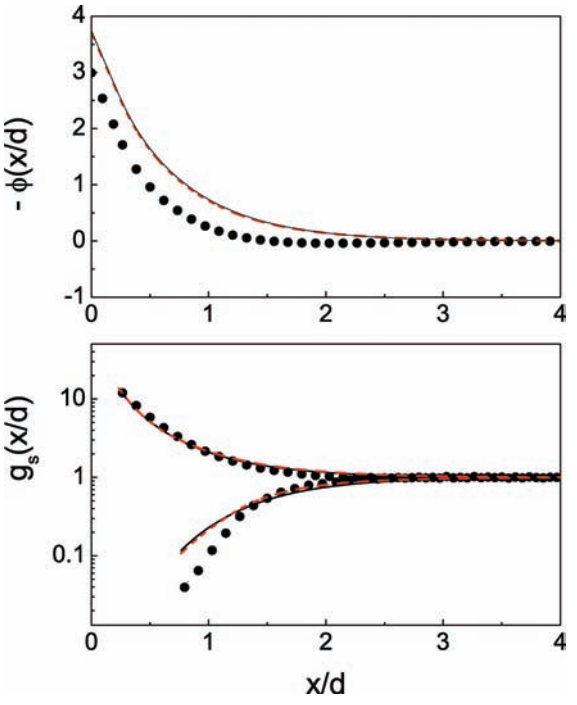

Figure 7. Mean electrostatic potential $\phi(x/d)$ and the electrode−ion singlet distribution functions $g_s(x/d)$ in a 1^+:2^- PM planar double layer at $\alpha = 0.308$, $\rho^* = 0.0875$ ($c = 0.5$ mol·dm^{-3}), $T^* = 0.297$ ($T = 298$ K), $b = 4$, and $\sigma^* = -0.229$ ($\sigma = -0.203$ C·m^{-2}). Notation as in Figure 4.

valency of the counterions, and this feature alone leads to the substantial differences in the structures observed.

The GCS profiles are all monotonic and do not show oscillations, which is only to be expected as the theory neglects both interionic correlations and exclusion effects. Although the exclusion volume corrected version of the theory, namely, the PB+EVT gives results that are close to the GCS results, in Figure 1 the PB+EVT counterion profile shows a slight shoulder. This trend is indicative of the potential usefulness of the PB +EVT theory at high concentrations. The MPB predictions, which further incorporate the ionic correlations through the fluctuation potential terms, in contrast, follow the MC simulation data very closely and are very nearly quantitative with the simulations. Earlier MPB calculations on 1:2/2:1 electrolytes have shown similar patterns.[26,27] In Figure 3, $T = 150$ K was used to see the effects of a temperature different from the room temperature. The parameters $T^* = 0.150$ ($T = 150$ K), $\rho^* = 0.0277$ ($c = 0.2$ mol·dm^{-3}), and $\sigma^* = -0.129$ ($\sigma = -0.114$ C·m^{-2}) are all relatively smaller in magnitude, and the simulation profiles are monotonic. The GCS and PB+EVT results are now much closer to the simulation values.

We next turn to asymmetric sized ions but with symmetric valencies. These results are given in Figures 4 to 6 at radius ratio $\alpha = 0.308$ and $b = 6$. The plots in Figures 4 and 5 are at $\rho^* = 0.170$ ($c = 1$ mol·dm^{-3}), $|\sigma^*| = 0.397$ ($|\sigma| = 0.352$ C·m^{-2}), and $T^* = 0.595$ ($T = 298$ K), while those in Figure 6 are at $\rho^* = 0.0851$ ($c = 0.5$ mol·dm^{-3}), $\sigma^* = 0.281$ ($\sigma = 0.249$ C·m^{-2}), and $T^* = 0.150$ ($T = 298$ K). Further, in Figure 4, $\sigma^* < 0$, and in Figure 5, $\sigma^* > 0$. Although the results shown in these three figures are all at $T = 298$ K, Figures 4 and 5 are for 1:1 systems and Figure 6 for a 2:2 system, and hence the difference in T^*. It is of interest to note that, with the values of d and ε_r used, $T^* = 0.15$ corresponds

dx.doi.org/10.1021/je2005193 |J. Chem. Eng. Data 2011, 56, 4556–4563

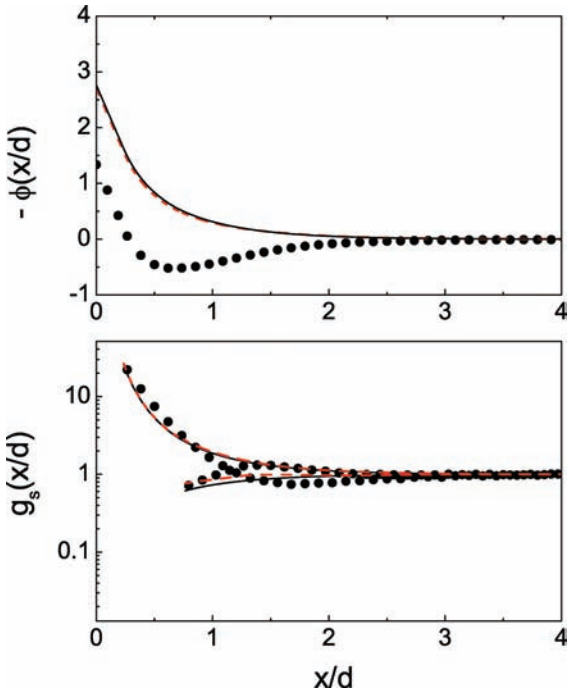

Figure 8. Mean electrostatic potential $\phi(x/d)$ and the electrode−ion singlet distribution functions $g_s(x/d)$ in a 2^+:1^- PM planar double layer at $\alpha = 0.308$, $\rho^* = 0.168$ ($c = 0.5$ mol·dm^{-3}), $T^* = 0.297$ ($T = 298$ K), $b = 4$, and $\sigma^* = -0.229$ ($\sigma = -0.203$ C·m^{-2}). Notation as in Figure 4.

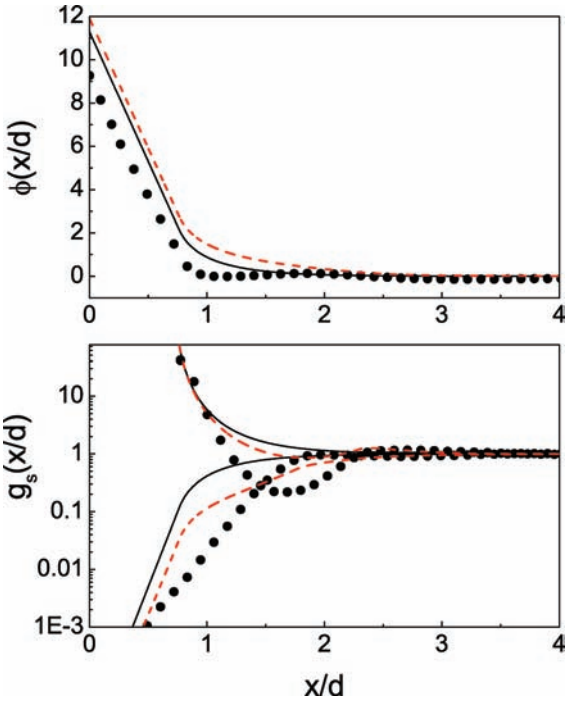

Figure 9. Mean electrostatic potential $\phi(x/d)$ and the electrode−ion singlet distribution functions $g_s(x/d)$ in a 1^+:2^- PM planar double layer at $\alpha = 0.308$, $\rho^* = 0.175$ ($c = 1$ mol·dm^{-3}), $T^* = 0.297$ ($T = 298$ K), $b = 7$, and $\sigma^* = 0.567$ ($\sigma = 0.503$ C·m^{-2}). Notation as in Figure 4.

to ∼300 K for a 2:2 valency system, which is the room temperature, whereas for a 1:1 valency system the same T^* would correspond to ∼75 K, a rather low temperature!

We note that, although the magnitudes of the physical parameters in Figures 4 and 5 are the same, there are qualitative differences in the results. The reason for this can be traced to the fact that the counterions are the smaller species in the former but the bigger species in the latter case. While the profiles are all smooth and monotonic in Figure 4, steric effects begin to be dominant with the bigger counterions leading to the layering[32,36,49,50] seen in the counterion profile in Figure 5. The close proximity of the smaller counterions to the electrode results in a steeper fall in the potential profile and a thinner double layer in Figure 4. This again shows the influence of the electrode−counterion interaction in the formation of the double-layer structure since now the different distances of closest approach of the co- and counterions to the electrode is the only distinguishing feature between the two systems. The MGCS and the PB+EVT results are close and qualitative with the simulations in Figure 4. Interestingly, in Figure 5 the PB+EVT results are still qualitative with the MC data and show the layering effect. The increased correlations with the multivalent ions lead to oscillations in the profiles in Figure 6 with the $\phi(x/d)$ changing sign before going to zero. The mean-field MGCS and PB+EVT distributions remain monotonic in this situation.

The results for a fully asymmetric electrolyte, in both ionic size and valency, are presented in the remaining set of figures (Figures 7 to 10). In all of the cases the $T^* = 0.297$ ($T = 298$ K) and the magnitudes of the valencies are in the ratio 1:2 with the cationic species being the smaller species. The radius ratio $\alpha = 0.308$ is mostly used except in Figure 10 where $\alpha = 0.545$. The physical difference between the model systems in Figure 7 ($\rho^* = 0.0875$ ($c = 0.5$ mol·dm^{-3}), $b = 4$, $\sigma^* = -0.229$ ($\sigma = 0.203$ C·m^{-2})) and Figure 8 ($\rho^* = 0.168$ ($c = 0.5$ mol·dm^{-3}), $b = 4$, $\sigma^* = -0.229$ ($\sigma = -0.203$ C·m^{-2})) is that the counterions are monovalent in the former case and divalent in the latter case. Since the counterions are also the smaller cationic species in both the situations, there are twice as many larger sized anionic co-ions in Figure 8 and hence the greater value of ρ^*. The influence of the electrode−counterion interaction is again manifest in the profile patterns: in Figure 7 the distributions are smooth with only a hint of faint oscillations, while in Figure 8 the oscillations are more clearly visible, and a minimum occurs in $\phi(x/d)$. The two mean field results are fairly close together in both the figures.

The salt concentration and the electrode surface charge are substantially increased in the double-layer systems of Figure 9 ($\rho^* = 0.175$ ($c = 1$ mol·dm^{-3}), $b = 7$, $\sigma^* = 0.567$ ($\sigma = 0.503$ C·m^{-2})) and 10 ($\rho^* = 0.217$ ($c = 1$ mol·dm^{-3}), $b = 7$, $\sigma^* = 0.567$ ($\sigma = 0.503$ C·m^{-2})), and the corresponding profiles now show more features. Note again the different values of ρ^* for the same value of the concentration for similar reasons as before. Although the smaller cationic co-ions are closer to the electrode, the dominance of the counterions (anions in these cases) is still evident. For example, the multivalent counterions are associated with a sharp fall in $\phi(x/d)$, oscillations in the profiles, and a thin, compact double layer in Figure 9. On the other hand monovalent counterions together with multivalent co-ions yield a more diffuse double layer in Figure 10. The overall picture that emerges regarding the relative influence of electrode−counterion interaction in these structures (Figures 7 to 10) is in line with that seen earlier for asymmetric valencies only or asymmetric-ion sizes only. For the fully asymmetric case of course, there is greater potential for rich structural features.

The steric effects due to an excess number of bigger sized counterions in the system corresponding to Figure 10 cause

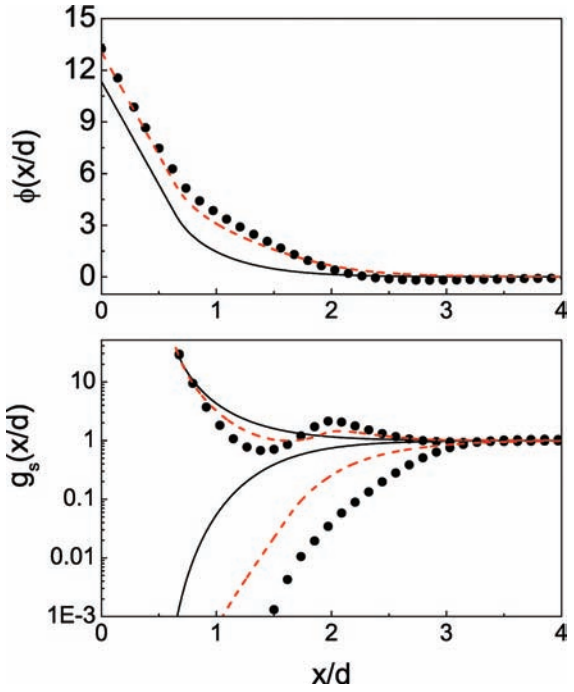

Figure 10. Mean electrostatic potential $\phi(x/d)$ and the electrode−ion singlet distribution functions $g_s(x/d)$ in a 2^+:1^- PM planar double layer at $\alpha = 0.545$, $\rho^* = 0.217$ ($c = 1$ mol·dm^{-3}), $T^* = 0.297$ ($T = 298$ K), $b = 7$, and $\sigma^* = 0.567$ ($\sigma = 0.503$ C·m^{-2}). Notation as in Figure 4.

layering in the electrode−counterion distributions. It ought to be emphasized that these results are at $\alpha = 0.545$, so that presumably a smaller α, that is, a larger variation in ion sizes would make this layering even more substantial. The PB+EVT profiles can undulate in contrast to their MGCS counterparts, reproduce layering, and lie closer to the simulation data in Figure 10. One final remark is in order. Because of the logarithmic scale used in displaying the electrode−ion singlet distributions, the differences between the MC simulations and the theories are exaggerated at small $g_s(x/d)$.

CONCLUSIONS

The main result of this paper has been an analysis of the evolution of structure in a PM planar double layer due to changing asymmetry in the electrolyte. We have treated asymmetry in (i) ionic valencies only, (ii) ionic sizes only, and (iii) both ionic valencies and sizes. A recurring feature running through the (density) profiles' pattern is the unmistakable evidence of the strong influence of the electrode−counterion interaction in characterizing double-layer structure. It has been known in the literature, for example, that, in a RPM double layer with (say) a positively charged electrode, 1^+:1^- and 2^+:1^- systems are structurally similar, as are 2^+:2^- and 1^+:2^- systems, with the counterions being charged alike in each instance. Our results reinforce such notions, and in particular for size-asymmetric ions the relative proximity of the counterions to the electrode is a further factor.

The RPM provides an illustration of the two basic phenomena which are not predicted by the classical GCS theory. First at a high electrode charge there can be a layering of counterions[32,36,49,50] at the electrode to balance the electrode charge. Not unexpectedly, the counterion layering is more pronounced in the presence of an excess of counterions, for example, when the magnitudes of the valencies of the co- and counterions are 2 and 1, respectively. Second at high electrolyte concentrations a charge reversal, or overcharging, can occur in the diffuse double layer that arises from a subtle combination of ion correlations and ion size. In particular, the mean electrostatic potential profile changes sign before becoming zero at large distances from the electrode. The onset of the behavior depends on the valency of the counterions. Both of these phenomena underlie the more complex structure of the electric double layer seen for different ion sizes.

Higher valency symmetric systems and/or asymmetric systems provide a more stringent challenge to a theory, and we find that, of the theories, none of the above effects is captured by the classical GCS or the MGCS theory, which are generally poor except at rather low salt concentrations. This is not surprising in view of the missing fluctuation potential (interionic correlations) and exclusion volume terms in the classical approach. The MPB theory, on the other hand, tries to incorporate such effects and is seen to be quite successful in reproducing the simulation results for the RPM systems. A more accurate version of the theory, is, however, required for asymmetric ion sizes.[48] The PB+EVT theory is geared to highly concentrated solutions when the exclusion volume effects are expected to dominate. Indeed, substantial qualitative differences between the GCS (or the MGCS) and the PB+EVT can occur at higher concentrations.

AUTHOR INFORMATION

Corresponding Author

*E-mail: doug@chem.byu.edu.

Funding Sources

L.B.B. acknowledges an institutional grant through Fondos Institucionales Para la Investigacion (FIPI), University of Puerto Rico.

ACKNOWLEDGMENT

One of the authors, Doug Henderson, has had a long, pleasant, and fruitful interaction with Ken Marsh dating back to 1967 when Ken and Doug were visitors at the CSIRO Division of Physical Chemistry, Fisherman's Bend, Melbourne, Australia, and more recently during Ken's tenure as Editor of this journal.

REFERENCES

(1) Nagy, T.; Valiskó, M.; Henderson, D.; Boda, D. Behavior of 2:1 and 3:1 electrolytes at polarizable interfaces. *J. Chem. Eng. Data* **2011**, *56*, 1316–1322.

(2) Gouy, M. Sur la constitution de la charge electrique a la surface d'un electrolyte. *J. Phys. (Paris)* **1910**, *9*, 457–468.

(3) Chapman, D. L. A contribution to the theory of electrocapillarity. *Philos. Mag.* **1913**, *25*, 475–481.

(4) Stern, O. Zur theorie der electrolytischen doppelschicht *Z. Elektrochem.* **1924**, *30*, 508–516.

(5) Torrie, G. M.; Valleau, J. P. The electrical double layer. III. Modified Gouy-Chapman theory with unequal sizes. *J. Chem. Phys.* **1982**, *76*, 4623–4630.

(6) Bhuiyan, L. B.; Blum, L.; Henderson, D. The application of the modified Gouy-Chapman theory to an electrical double layer containing asymmetric ions. *J. Chem. Phys.* **1983**, *78*, 442–445.

(7) Blum, L. Theory of electrified interfaces. *J. Phys. Chem.* **1977**, *81*, 136–147.

(8) Carnie, S. L.; Chan, D. Y. C.; Mitchell, D. J.; Ninham, B. W. The structure of electrolytes at charged surfaces; the primitive model. *J. Chem. Phys.* **1981**, *74*, 1472–1478.

(9) Lozada-Cassou, M.; Saavedra-Barrera, R.; Henderson, D. The application of the hypernetted chain approximation to the electrical double layer. Comparison with Monte Carlo results for symmetric salts. *J. Chem. Phys.* **1982**, *77*, 5150–5156.

(10) Plischke, M.; Henderson, D. Pair correlation functions and density profiles in the primitive model electric double layer. *J. Chem. Phys.* **1988**, *88*, 2712–2718.

(11) Plischke, M.; Henderson, D. Pair correlation functions and the structure of the electric double layer. *Electrochim. Acta* **1989**, *34*, 1863–1867.

(12) Kjellander, R.; Marčelja, S. Inhomogeneous Coulomb fluids with image interactions between planar surfaces. 1. *J. Chem. Phys.* **1985**, *82*, 2122–2135.

(13) Greberg, H.; Kjellander, R. Electric double layer properties calculated in the anisotropic reference hypernetted chain approximation. *Mol. Phys.* **1994**, *83*, 789–801.

(14) Di Caprio, D.; Valiskó, M.; Holovko, M.; Boda, D. Anomalous temperature dependence of the differential capacitance in valence asymmetric electrolytes. Comparison of Monte Carlo simulation results and the field theoretical approach. *Mol. Phys.* **2006**, *104*, 3777–3786.

(15) Di Caprio, D.; Valiskó, M.; Holovko, M.; Boda, D. Simple extension of a field theory approach for the description of the double layer accounting for excluded volume effects. *J. Phys. Chem. C* **2007**, *111*, 15700–15705.

(16) Boda, D.; Fawcett, W. R.; Henderson, D.; Sokolowski, S. Monte Carlo, density functional theory, and Poisson-Boltzmann theory study of the structure of an electrolyte near an electrode. *J. Chem. Phys.* **2002**, *116*, 7170–7176.

(17) Gillespie, D.; Valiskó, M.; Boda, D. Density functional theory of the electrical double layer: the RFD functional. *J. Phys.: Condens. Matter* **2005**, *17*, 6609–6626.

(18) Gillespie, D.; Nonner, W; Eisenberg, R. Coupling Poisson-Nernst-Planck and density functional theory to calculate ionic flux. *J. Phys.: Condens. Matter* **2002**, *14*, 12129–12145.

(19) Valiskó, M.; Boda, D.; Gillespie, D. Selective adsorption of ions with different diameter and valence at highly charged interfaces. *J. Phys. Chem. C* **2007**, *111*, 15575–15585.

(20) Wang, K.; Yu, Y.-X.; Gao, G.-H.; Luo, G.-S. Density functional theory and Monte Carlo simulation study on the electric double layer around DNA in mixed size counterion systems. *J. Chem. Phys.* **2005**, *123*, 234904−1–234904−11.

(21) Yu, Y.-X.; Wu, J.; Gao, G.-H. Ionic distribution, electrostatic potential, and zeta potential at electrochemical interfaces. *Chinese J. Chem. Eng.* **2004**, *12*, 688–695.

(22) Pizio, O.; Patrykiejew, A.; Sokolowski, S. Phase behaviour of ionic fluids in slit-like pores: A density functional approach for the restricted primitive model. *J. Chem. Phys.* **2004**, *121*, 11957–11964.

(23) Martin-Molina, A.; Hidalgo-Álvarez, R.; Quesada-Perez, M. Additional considerations about the role of ion size in charge reversal. *J. Phys.: Condens. Matter* **2009**, *21*, 424105−1–424105−7.

(24) Guerrero-Garcia, G. I.; González-Tovar, E.; Chávez-Páezá, M.; Lozada-Cassou, M. Overcharging and charge reversal in the electrical double layer around the point of zero charge. *J. Chem. Phys.* **2010**, *132*, 054903−1–054903−19.

(25) Kiyohara, K.; Sugino, T.; Asaka, K. Electrolytes in porous electrodes: Effects of the pore size and the dielectric constant of the medium. *J. Chem. Phys.* **2010**, *132*, 144705−1–144705−12.

(26) Outhwaite, C. W.; Bhuiyan, L. B. An improved modified Poisson-Boltzmann equation in the electric double layer theory. *J. Chem. Soc., Faraday Trans. 2* **1983**, *79*, 707–718.

(27) Bhuiyan, L. B.; Outhwaite, C. W. Comparison of the modified Poisson-Boltzmann theory with recent density functional theory and simulation results in the planar electric double layer. *Phys. Chem. Chem. Phys.* **2004**, *6*, 3467–3473.

(28) Bhuiyan, L. B.; Outhwaite, C. W. Comparison of density functional and modified Poisson-Boltzmann structural properties for a spherical double layer. *Condens. Matter Phys.* **2005**, *8*, 287–302.

(29) Patra, C. N.; Bhuiyan, L. B. The effect of ion size on polyion-small ion distributions in a cylindrical double layer. *Condens Matter Phys.* **2005**, *8*, 425–446.

(30) Bhuiyan, L. B.; Outhwaite, C. W. Comparison of exclusion volume corrections to the Poisson-Boltzmann equation for inhomogeneous electrolytes. *J. Colloid Interface Sci.* **2009**, *331*, 543–547.

(31) Silvestre-Alcantara, W.; Bhuiyan, L. B.; Outhwaite, C. W.; Henderson, D. A modified Poisson-Boltzmann study of the singlet ion distribution function at contact with the electrode for a planar electric double layer. *Collect. Czech. Chem. Commun.* **2010**, *75*, 425–446.

(32) Torrie, G. M.; Valleau, J. P. Electrical double layers. I. Monte Carlo study of a uniformly charge surface. *J. Chem. Phys.* **1980**, *73*, 5807–5816.

(33) Torrie, G. M.; Valleau, J. P. Electrical double layers. 4. Limitations of the Gouy-Chapman theory. *J. Phys. Chem.* **1982**, *86*, 3251–3257.

(34) Boda, D.; Chan, K.-Y.; Henderson, D. Monte Carlo study of the capacitance of the double layer in a molten salt. *J. Chem. Phys.* **1999**, *110*, 5346–5350.

(35) Boda, D.; Henderson, D.; Chan, K.-Y.; Wasan, D. Low temperatures anomalies in the properties of the electrochemical double layer. *Chem. Phys. Lett.* **1999**, *308*, 473–478.

(36) Lamperski, S.; Bhuiyan, L. B. Counterion layering at high surface charge in an electric double layer. Effect of local concentration approximation. *J. Electroanal. Chem.* **2003**, *540*, 79–87.

(37) Bhuiyan, L. B.; Outhwaite, C. W.; Henderson, D. Planar electric double layer for a restricted primitive model electrolyte at low temperatures. *Langmuir* **2006**, *22*, 10630–10634.

(38) Bhuiyan, L. B.; Outhwaite, C. W.; Henderson, D. Some simulation and modified Poisson-Boltzmann theory results for the contact values of an electrolyte near acharged electrode. *J. Electroanal. Chem.* **2007**, *607*, 54–60.

(39) Bhuiyan, L. B.; Outhwaite, C. W.; Henderson, D.; Alawneh, M. A further Monte Carlo and modified Poisson-Boltzmann analysis of two recent results in the electric double layer theory. *Bangladesh J. Phys.* **2007**, *4*, 93–102.

(40) Bhuiyan, L. B.; Outhwaite, C. W.; Henderson, D. Evidence from Monte Carlo simulations for a second contact value theorem for a double layer formed by 2:1/1:2 salts at low electrode charges. *Mol. Phys.* **2009**, *107*, 342–347.

(41) Bhuiyan, L. B.; Henderson, D. A local semi-empirical contact condition for the charge profile in an electric double layer with size-asymmetric ions at low electrode charge. *Mol. Simul.* **2011**, *37*, 269–276.

(42) Bhuiyan, L. B.; Henderson, D. Evidence for a second, local contact condition for a planar electric double layer containing size and valencey asymmetric ions. *Mol. Phys.* **2011**, in press.

(43) Bhuiyan, L. B.; Henderson, D. Evidence for a second contact value theorem for the electric double layer. *Mol. Simul.* **2007**, *33*, 935–957.

(44) Boda, D.; Chan, K.-Y.; Henderson, D. Monte Carlo simulation of an ion-dipole mixture as a model of an electrical double layer. *J. Chem. Phys.* **1998**, *109*, 7362–7371.

(45) Fischer, J. A fluid in contact with a wall. The Percus-Yevick versus the superposition approximation. *Mol. Phys.* **1977**, *33*, 75–81.

(46) Lebowitz, J. L. Exact solution of generalized Percus-Yevick equation for a mixture of hard spheres. *Phys. Rev.* **1964**, *133*, A895–A899.

(47) Outhwaite, C. W.; Bhuiyan, L. B.; Levine, S. Theory of the electric double layer using a modified Poisson-Boltzmann equation. *J. Chem. Soc., Faraday Trans. 2* **1980**, *16*, 1388–1408.

(48) Outhwaite, C. W.; Bhuiyan, L. B. A modified Poisson-Boltzmann equation in electric double layer theory for a primitive model electrolyte with size-asymmetric ions. *J. Chem. Phys.* **1986**, *84*, 3461–3471.

(49) Nielaba, P.; Forstmann, F. Packing of ions near an electrolyte-electrode interface in the HNC/LMSA approximation to the RPM model. *Chem. Phys. Lett.* **1985**, *117*, 46–48.

(50) Lamperski, S.; Outhwaite, C. W. Exclusion volume term in the inhomogeneous Poisson-Boltzmann theory for high surface charge. *Langmuir* **2002**, *18*, 3423–3424.